TOTAL DEGRADATION ANALYSIS OF PRECODED SIGNALS ONTO NON-LINEAR SATELLITE CHANNELS

Danilo Spano*, Dimitrios Christopoulos*, Stefano Andrenacci*, Symeon Chatzinotas*, Jens Krause**, and Björn Ottersten*

*Interdisciplinary Centre for Security, Reliability and Trust (SnT), University of Luxembourg
4, rue Alphonse Weicker, L-2721 Luxembourg
Email: {danilo.spano, dimitrios.christopoulos, stefano.andrenacci, symeon.chatzinotas, bjorn.ottersten}@uni.lu

**SES S.A., Château de Betzdorf, L-6815 Betzdorf
Email: jens.krause@ses.com

Abstract

Linear precoding exploits the spatial degrees of freedom offered by multi-antenna transmitters to manage interferences between multiple co-channel users. The adoption of precoding in practical systems, however, entails a series of practical barriers. Amongst several issues, the focus herein is on the non-linear dependence of the input versus the output power of the efficient and reliable amplifiers that drive each transmit antenna, which limits the system performance. As a first step, the present work studies the impact of linear precoding on the peak-to-average power ratio (PAPR) of precoded waveforms in multibeam satellite systems using a finite alphabet. In this context, a sensitivity analysis of the PAPR at the input of each amplifier with respect to intrinsic system level parameters, such as the number of transmit feeds, is performed. Next, the performance of the whole non-linear satellite chain is analyzed with respect to the symbol-error-rate (SER) and the total degradation (TD) of the channel. Furthermore, two low-complexity solutions are considered for counteracting the effects of the non-linearities of the satellite channel on the precoded waveforms, namely an automatic gain control (AGC) operation and a non-linear equalization performed at the receiver side.

1. Introduction

Multi-user multiple-antenna transmitters are the way forward towards the high throughput next generation systems. In this direction, advanced transmit signal processing techniques have been included in the most recent extensions of broadband multibeam satellite communication (SatCom) standards [1]. Their goal is to optimize the performance of the multibeam satellites while keeping the complexity of the receiver reasonable. A fundamental requisite for the application of these techniques, referred to as linear precoding, is the knowledge of the channel state information (CSI) at the transmitter. Subsequently, the exploitation of the spatial degrees of freedom offered by the antenna array mitigates the multi-user interference (MUI), thus allowing co-channel beams to be made adjacent. In this fashion, a spatial division multiple access (SDMA) scheme is realized. Channel based linear precoding has shown great potential for satellite systems [2], [3]. Therefore, recent works have taken precoding over satellite to the next level. To account for practical system implementations, the consideration of precoding on a frame-by-frame basis has been presented in [4], [5]. In this framework, the notion of frame-based precoding has been established [6]. Nevertheless, all the above mentioned works fail to acknowledge the non-linear amplification carried out over the satellite. The non-linear channel impairments, resulting in a distortion of the transmitted signals, have been tackled in the literature in different ways, based on peak-to-average power ratio (PAPR) reduction [7], on specific precoding techniques [8], and on predistortion techniques [9], [10]. The present work, however, takes a step backward and aims at evaluating the effects of a practical satellite channel on generic linear precoded signals. Differently from the previous works, we focus here on low-complexity solutions: an automatic gain control (AGC) stage properly set for precoded waveforms, and a non-linear equalization scheme.

2. System Model

The focus is on a multi-user (MU) multiple-input multiple-output (MIMO) satellite system. The on-board

antenna of a satellite comprises a parabolic reflector and an array of feeds, which allows to generate multiple independent beams. Let N_t denote the number of transmitting elements of the transmitter and K the number of users. We consider a system with a single feed, carrier and high-power amplifier (HPA) per beam. Let us also assume that $K = N_t$, namely considering one user per beam in a specific instant. This is reasonable if the system resorts to a time-division multiplexing (TDM) scheme in order to serve all the users in each beam, which results in a single user per beam per time-slot. The received signal at user i will be $y_i = \boldsymbol{h}_i^{\dagger}\boldsymbol{x} + n_i$, where $\boldsymbol{h}_i \in \boldsymbol{C}^{N_t \times 1}$ contains the channel coefficients (amplitude and phase) related to i-th user, $(\cdot)^{\dagger}$ is the conjugate transpose operator, $\boldsymbol{x} \in \boldsymbol{C}^{N_t \times 1}$ is the transmitted signal, and n_i is a complex circular symmetric random variable, modeling the zero mean Additive-White-Gaussian-Noise (AWGN) measured at the i-th user's receive antenna. Let us denote by $\boldsymbol{w}_i \in \boldsymbol{C}^{N_t \times 1}$ the precoding vector applied to the transmit antennas to beamform towards the i-th user. By collecting all the precoder vectors in a precoder matrix $\boldsymbol{W} = [\boldsymbol{w}_1 \dots \boldsymbol{w}_K] \in \boldsymbol{C}^{N_t \times K}$, and all the channel vectors in a channel matrix $\boldsymbol{H} = [\boldsymbol{h}_1 \dots \boldsymbol{h}_K]^{\dagger} \in \boldsymbol{C}^{N_t \times K}$, the input-output relation of the system can be rewritten as

$$\boldsymbol{y} = \boldsymbol{H}\boldsymbol{W}\boldsymbol{s} + \boldsymbol{n}, \tag{1}$$

where, in turn, $\boldsymbol{s} \in \boldsymbol{C}^{K \times 1}$ collects the symbols transmitted to the users, $\boldsymbol{n} \in \boldsymbol{C}^{K \times 1}$ collects the AWGN independent identical distributed (i.i.d.) components related to the users, and $\boldsymbol{y} \in \boldsymbol{C}^{K \times 1}$ the corresponding received signals at the users. It is important to highlight that, based on DVB-S2X standard [1], finite alphabets will be considered for the transmitted symbols.

As regard to the channel model, assuming fixed users with highly directive antennas, we consider real channel gains depending only on the multibeam antenna pattern and on the users position[1]. Considering the i-th beam and the k-th user, the corresponding entry of the channel matrix $\boldsymbol{H}$ can be calculated resorting to the well accepted method of Bessel functions, thus it will be the square root of [3]

$$g_{ik}(\theta_{ik}) = G_{\max}\left(\frac{J_1(u)}{2u} + 36\frac{J_3(u)}{u^3}\right)^2, \tag{2}$$

where θ_{ik} is the off-axis angle of the user with respect to the boresight of the beam, $u = 2.07123\sin(\theta_{ik}) / \sin(\theta_{3dB})$, $G_{\max}$ is the maximum axis gain of the antenna, and J_1, J_3 are the Bessel functions of the first kind, of order one and three respectively.

As to the precoding method, in this work we resort to the well-known zero-forcing (ZF) technique [2] which, inverting the channel matrix, allows to fully cancel out the MUI, though showing limitations in a noise-limited scenario. Since the scenario at hand is interference-limited, due to full frequency reuse in the antenna pattern, ZF precoding is a suitable technique. Because we assumed that $K = N_t$, the ZF precoder will read simply as $\boldsymbol{W} = \boldsymbol{H}^{-1}$, while in a more general case (here not considered just for simplicity) it would be the pseudo-inverse of the channel matrix.

As regard to the practical per-beam power constraints for the transmitting antennas, they are taken into account by simply re-scaling the precoded signals, in order to respect the tightest power constraint at the transmitting feeds. Although this is not an optimal approach, it provides a low-complexity solution for the model at hand.

2.1. Non-linearity of the Satellite Channel

The non-linearity of the satellite channel, which results in a deterioration of the transmitted precoded signals, is introduced by the non-ideal on-board amplification stage. Indeed, the signals feeding the on-board traveling-wave-tube amplifiers (TWTAs) are subject to a non-linear effect, which affects both the amplitude and the phase. Considering the non-linearized TWTA model defined in [11] (this is a static model, not taking into account memory effects of the TWTA), the corresponding amplitude-to-amplitude (AM-AM) and amplitude-to- phase (AM-PM) characteristics are shown in Fig. 1. These curves represent the relationship between the input and the output power of the amplifier, and between the input power and the output phase shift, respectively. The on-board TWTA needs to be operated as close as possible to saturation, to efficiently exploit the scarce available power. As clear from the curves, this drives the operating point to a region where the instantaneous output power is a non-linear function of the input power. This non-linear amplification, in particular when combined with channels that introduce memory,

[1] However, the main conclusions of this work are still valid if a random phase is incorporated in the channel model.

leads to signal distortion. In the remainder of this work, the effects of this non-linear amplification on the precoded waveforms are investigated, based on simulations. To this end, a relevant parameter that is analysed is the PAPR of the transmitted signals.

For the sake of clarity, Fig. 2 displays the overall block scheme of the simulated satellite forward link. As shown in the scheme, in the ground segment, after the mapping of each bit stream into a symbol stream according to a specific modulation, a pilot sequence (P2) is attached to the payload. The P2 pilot sequence, present in the DVB-S2X super-frame structure [1], is a sequence of 180 symbols, known at the receiver side, which is modulated and precoded as the information sequence. Such characteristics enable a receive equalization scheme, which will be described in the following. After the precoding module, each branch contains a square-root-raised-cosine (SRRC) filter for the shaping and the transmission of the signals.

The space segment, besides the described non-linear TWTAs, includes the blocks corresponding to the input multiplexer (IMUX) and the output multiplexer (OMUX). Moreover, an AGC scheme is considered before the amplification stage. Such component, fundamental for handling the non-linearity issue, will be described in the following.

Finally, after the satellite channel, the user segment branches include the mentioned equalization block and the demapper, which returns the information symbols.

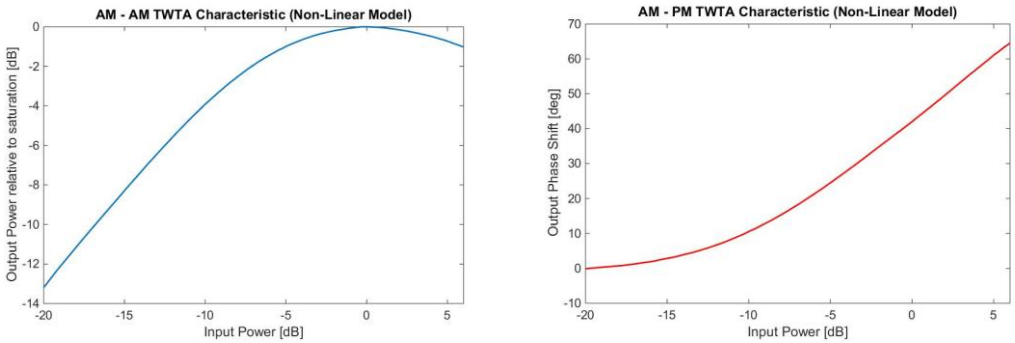

Figure 1: Input-Output characteristics of the on-board TWTA (AM-AM and AM-PM).

3. Performance Analysis and Proposed Solutions

3.1. PAPR Analysis

A first evaluation of the effect of the channel non-linearities onto the precoded waveforms can be given by studying the PAPR of the transmitted signals. Considering ZF precoding, Fig. 3 shows how the PAPR increases with the number of feeds of the multibeam antenna, both for precoded and non precoded waveforms. Moreover, the PAPR curves are shown in two cases, one considering a SRRC filtering operation (with a roll-off factor set to 0.25) and the other without. Therefore, the curves including filtering evaluate the signal in the sample domain, while the un-filtered in the symbol domain. The depicted curves are obtained according to the simulation chain of Fig. 2, and for each curve the corresponding point of the chain is mentioned (the curve assuming non precoded waveforms and filtering is derived after the SRRC block, but neglecting the precoder). The modulation scheme considered for these curves is 32-amplitude-phase-shift-keying (32-APSK). Analogous curves, here not reported for the sake of brevity, can be obtained considering different modulation orders. As one can easily envisage, the PAPR increases with the modulation order.

From such result, it can be seen that the precoded waveforms show a higher PAPR with respect to the non precoded ones. As a consequence, the distortion induced on the signals by the TWTA will be stronger when precoding is applied. Nevertheless, the percentage of the increase of PAPR in the sample domain is lower. Thus, we can deduce that the effect of precoding is not as detrimental if one considers a more accurate modeling of the transmission chain. These conclusions hold true if one considers different modulation orders, or a different roll-off factor in the filtering stage.

In addition to the increase of the PAPR for the precoded waveforms, it should be kept in mind that the channel distortion also affects the performance of precoding, leading to an imperfect compensation of the MUI. This is a further motivation for envisaging a stronger signal corruption when precoded is applied.

3.2. Effects of the Channel non-Linearities

In order to analyse the effects induced by the non-linearities of the satellite channel onto the precoded waveforms, it is worth considering the scatter plot representations of the transmitted symbols as

resulting by simulations, according to the block scheme of Fig. 2. However, at first the blocks referring to the AGC stage and to the non-linear equalization, which will be characterized in the remainder of this section, are not considered.

The following scatter plots are obtained by assuming a 32-APSK modulation scheme and a E_s/N_0 value (ratio of the average energy per symbol over the noise power spectral density) of 25 dB, on a 7-beam system using ZF precoding.

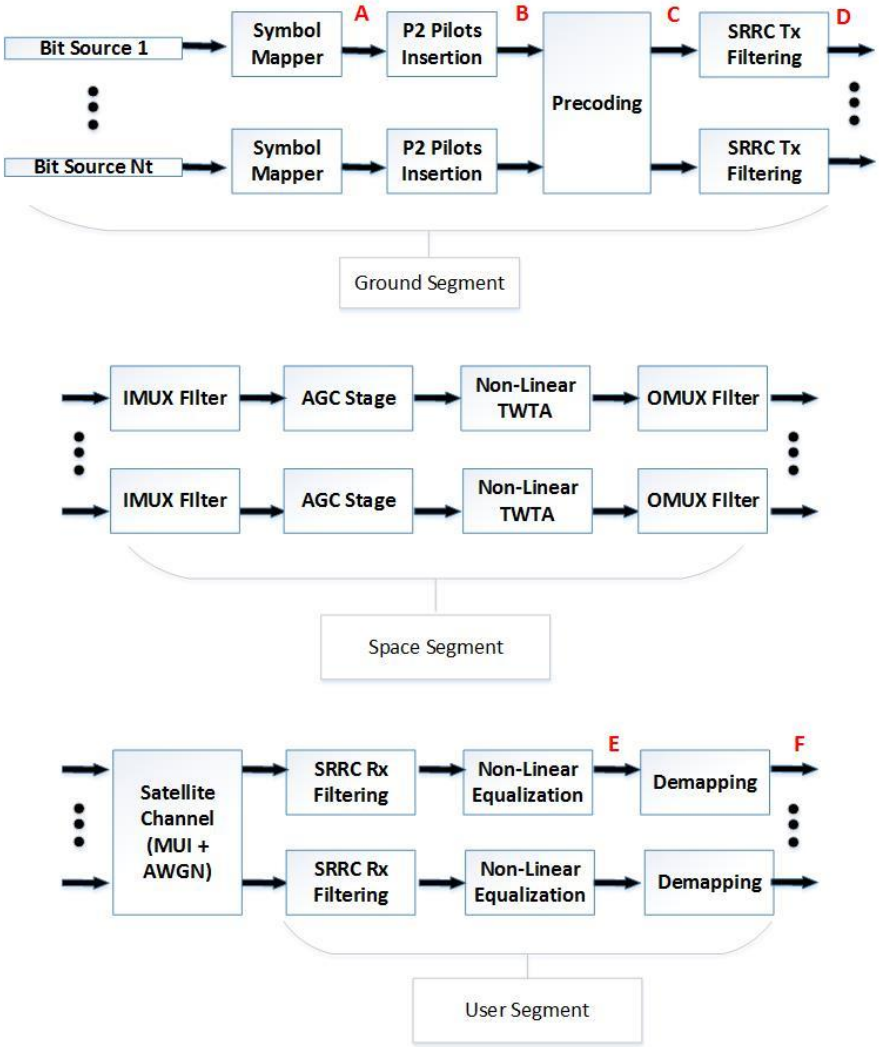

Figure 2: Block scheme of the considered satellite forward link.

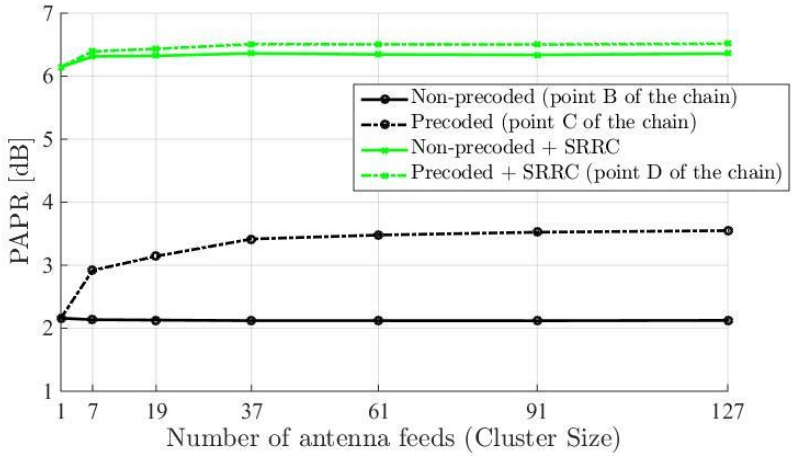

Figure 3: PAPR of 32-APSK signals vs. Number of transmitting elements.

First, Fig. 4 shows the transmitted symbols, for one of the data streams, before the precoding operation (left side) and after it (right side). It is visible how the precoding operation changes the constellations, correlating the different symbol streams according to Eq. 1 and therefore increasing the PAPR, as already discussed.

Then, in Fig. 5 the scatter plots of the received symbols are depicted, compared with the transmitted ones, both in the case of a linear AWGN channel, hence without the non-linear TWTA block (left side), and in the case including the channel non-linearities (right side). The deterioration of the transmitted precoded signals is highly visible in the second case. More specifically, we can observe two effects of the channel non-linearities on the received constellations [12]:

- a warping effect on the constellation centroids, due to the non-linear characteristics of the TWTA, which consists in a displacement of the centroids both in amplitude and in phase;
- a clustering effect on the received symbols, due to the inter-symbol interference (ISI), which is enhanced by the TWTA non-linearities.

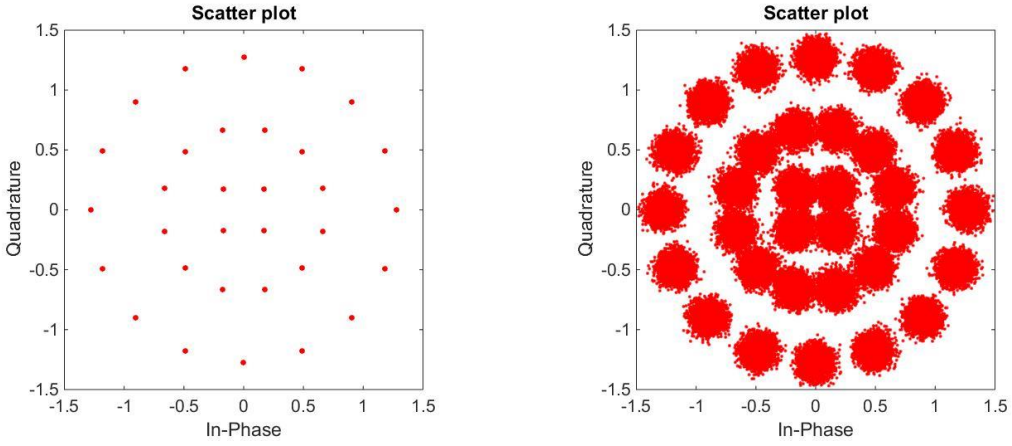

Figure 4: Tx constellations before (left - at point A of Fig. 2) and after (right - at point C of Fig. 2) precoding.

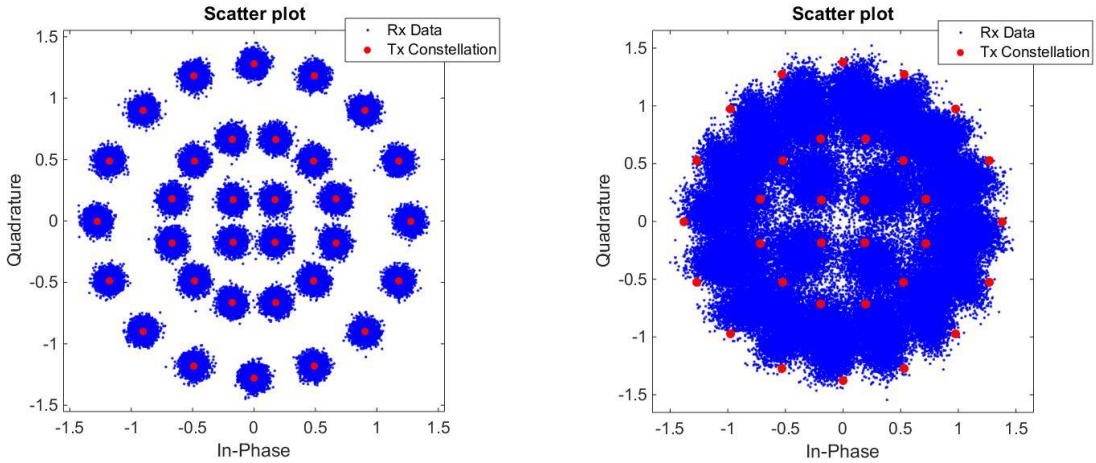

Figure 5: On the left, Scatterplots of the Tx and Rx constellations (at the points A and F of the chain, respectively), with a linear AWGN channel; on the right, same constellations with a non-linear satellite channel.

In the following section, we focus on two solutions aiming at counteracting the signal corruption due to the channel non-linearities.

3.2. Proposed Solutions

The investigated solutions are:

- a proper automatic gain control (AGC) stage [13], applying a power back-off to the transmitted signals so to reduce the distortion;
- a non-linear equalization module at the receiver, which aims at compensating the distortion induced by the TWTAs. This compensation is based on the transmission of a known sequence, i.e., a pilot sequence or a training sequence.

These techniques are meant as low-complexity solutions to the distortion induced by the on-board amplifiers, and can apply in general, since are not specific to systems relying on precoding.

The AGC stage applies to the signals an input back-off (IBO), which can be defined, in dB, as

$$IBO = 10\,\mathrm{Log}\left(\frac{P_{SAT}}{P_{AV}}\right),$$

where P_{SAT} represents the saturation power of the amplifier, whilst P_{AV} denotes the average signal power after the back-off operation. Such operation is depicted in Fig. 6, where the red mark represents the saturation point of the TWTA and the black mark is the operational point. It is clear how, at the cost of a reduced transmitted power, the distortion is reduced. The IBO value to be applied (equivalently, we can refer to the output back-off – OBO) has to be set in order to minimize the corruption of the transmitted signals. As shown in the next section concerning the numerical results, the optimization of the back-off value, for systems relying on ZF precoding, is performed numerically, based on the total degradation of the channel.

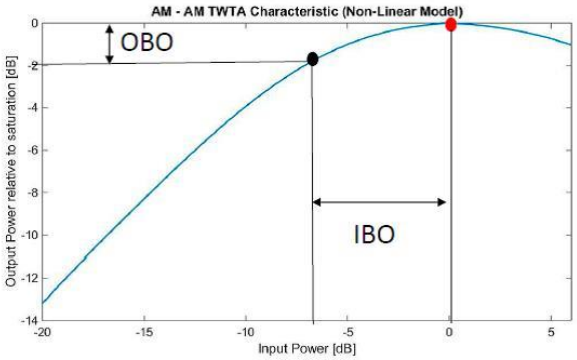

Figure 6: Back-off operation onto the transmitted useful power.

Concerning the non-linear equalization block introduced in the user segment, it leverages the P2 pilot sequence attached to the payload, previously mentioned. In particular, the received P2 sequence is used by the receiver for estimating the distortion suffered by the signals and, accordingly, for designing a new constellation to be used for demapping the received symbols. For determining the new (APSK) constellation, the rings amplitudes, as well as the relative phase shifts between the rings, are obtained using the received distorted version of the pilot symbols and exploiting the knowledge of their original transmitted version. More specifically, the detection regions of the new designed APSK constellation are calculated by averaging amplitudes and phases of the received pilots, on the corresponding levels.

3.2. Numerical Results

In order to show how the proposed chain of Fig. 2 behaves, with the inclusion of the AGC and non-linear equalization stages, some simulation results are reported hereafter. The results are obtained using the parameters listed in Tab.1.

Parameter	Value
Symbol Rate	25 MBaud
Number of Beams	7
Number of Tx Symbols	10^5
Modulation	32-APSK
Roll-off	0.3
IBO	3.6 - 5 dB
E_s/N_0	25 dB

Table 1: Simulation Parameters

Fig. 7 shows the scatter plot of the received constellation after demapping, obtained applying the AGC stage with an IBO of 5 dB. The black constellation represents the constellation used for demapping the received symbols, designed in the equalization stage. It is apparent how this constellation matches the received clouds better than the original one. The distortion on the symbols is still clearly visible in the clustering and warping effects. Nevertheless, they appear strongly mitigated with respect to the scatter plot of Fig. 5 (right side), resulting in a lower symbol-error-rate (SER).

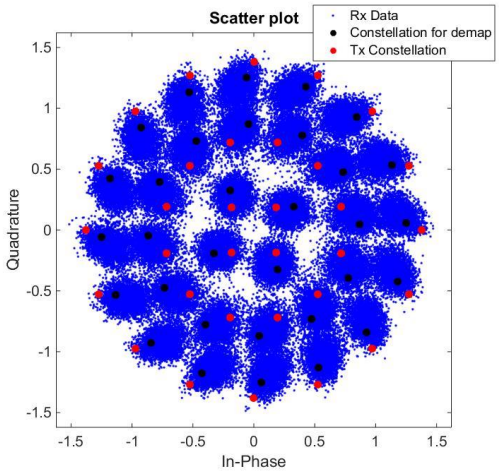

Figure 7: Scatterplots of the Tx and Rx constellations (at the points A and F of the chain, respectively), with an IBO of 5 dB and equalization at the Rx. The black constellation is available at the point E of the chain.

Concerning the SER obtained by applying the proposed solutions, Fig. 8 (left side) shows how it varies with the E_s/N_0 value, comparing the multibeam case, where ZF precoding is applied, with the single-beam case. The IBO is set to 3.6 dB. The result confirms how, in the precoded case, the system suffers more the effects of the channel non-linearities.

In Fig. 8 (right side) another important performance metric is considered for the system at hand. Such metric is given by the total degradation (TD) of the link, defined as [12] (all the quantities are in dB):

$$TD = \left(\frac{E_S}{N_0}\right)_{req}^{NL} - \left(\frac{E_S}{N_0}\right)_{req}^{AWGN} + OBO, \tag{3}$$

where $\left(\frac{E_S}{N_0}\right)_{req}^{NL}$ is the E_s/N_0 value required to achieve a predetermined target SER with the non-linear channel, $\left(\frac{E_S}{N_0}\right)_{req}^{AWGN}$ is the same quantity considering a linear AWGN channel, and OBO is the output power back-off. The OBO of the system has to be set in order to minimize the resulting total degradation. In Fig. 8 (right side) the TD curves, plotting the total degradation as a function of the OBO, are depicted, comparing the multibeam precoded case with the single-beam case. The TD curves are obtained assuming a target SER of 0.2, which, once using also some typical forward error correction (FEC) techniques, can lead to a quasi-error-free transmission. The optimum back-off corresponds to the minimum of the TD curves. As visible, also this result shows that in the multibeam precoded cases the degradation of the link is higher with respect to the single-beam case. In addition to this, the optimum back-off is about 0.7 dB higher in the multibeam case. Ultimately, we can identify a tradeoff between precoding, which allows for more spectrum per user link in multibeam systems, and the applied power back-off, which reduces the useful transmitted power.

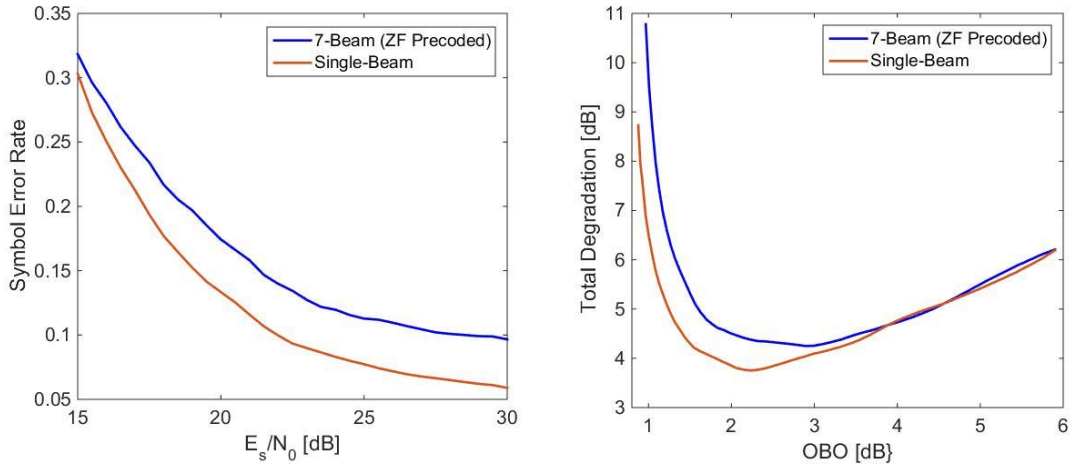

Figure 8: On the left, SER vs. E_s/N_0 curves, for the precoded and non-precoded cases; on the right, TD vs. OBO curves, comparing the same cases.

4. Conclusions

In this work we have studied the impact of the non-linearities of the satellite channel onto the performance of a multi-user satellite system relying on ZF precoding, introducing and validating some low-complexity solutions, based on power back-off and non-linear equalization. A performance analysis, based on the SER measured at the receiver side and on the total degradation of the satellite channel, has been performed. This analysis shows how the distortion induced by the channel has a greater effect, with respect to conventional systems, when precoding is applied. Consequently, higher OBO values are required in the AGC stage. Extension of the work shall account more advanced precoding techniques, such as the recent frame-based precoding [6], including also per-antenna power constraints, towards better utilizing the on-board available power [14]. Furthermore, other techniques will be considered for handling precoding onto non-linear channels, aiming at keeping all the complexity at the transmitter side. In this regard, innovative solutions based on predistortion combined with precoding, as well as on ad-hoc precoding techniques designed for non-linear channels, will be investigated.

Acknowledgement

This work was partially supported by the National Research Fund, Luxembourg under the projects SATSENT and SeMiGod.

References

[1] ETSI EN 302 307-2, “Digital video broadcasting (DVB); second generation framing structure, channel coding and modulation systems for broadcasting, interactive services, news gathering and other broadband satellite applications; part II: S2-extensions (S2X).”

[2] G. Zheng, S. Chatzinotas, and B. Ottersten, “Generic optimization of linear precoding in multibeam satellite systems,” *IEEE Trans. Wireless Commun.*, vol. 11, no. 6, pp. 2308 –2320, Jun. 2012.

[3] D. Christopoulos, S. Chatzinotas, G. Zheng, J. Grotz, and B. Ottersten, “Linear and non-linear techniques for multibeam joint processing in satellite communications,” *EURASIP J. on Wirel. Commun. and Networking 2012, 2012:162*. [Online]. Available: http://jwcn.eurasipjournals.com/content/2012/1/162

[4] D. Christopoulos, P.-D. Arapoglou, S. Chatzinotas, and B. Ottersten, “Linear precoding in multibeam satcoms: Practical constraints,” in *31st AIAA International Communications Satellite Systems Conference (ICSSC)*, Florence, IT, Oct. 2013.

[5] G. Taricco, “Linear precoding methods for multi-beam broadband satellite systems,” in *European Wireless 2014; 20th European Wireless Conference; Proceedings of*, May 2014, pp. 1–6.

[6] D. Christopoulos, S. Chatzinotas, and B. Ottersten, “Multicast multigroup precoding and user scheduling for frame-based satellite communications,” *Wireless Communications, IEEE Transactions on*, vol. PP, no. 99, pp. 1–1, 2015.

[7] S. H. Han and J. H. Lee, “An overview of peak-to-average power ratio reduction techniques for multicarrier transmission,” *Wireless Communications, IEEE*, vol. 12, no. 2, pp. 56–65, April 2005.

[8] Dantona, V., Delamotte, T., Bauch, G., Lankl, B., "Impact of nonlinear power amplifiers on the performance of precoded MIMO satellite systems," in *Satellite Telecommunications (ESTEL), 2012 IEEE First AESS European Conference on*, vol., no., pp.1-7, 2-5 Oct. 2012.

[9] Y. Cheng and M. Pesavento, “Predistortion and precoding vector assignment in codebook-based downlink beamforming,” in *Signal Processing Advances in Wireless Communications (SPAWC), 2013 IEEE 14th Workshop on*, June 2013, pp. 445– 449.

[10] M. Alvarez-Diaz, C. Mosquera, M. Neri, and G. Corazza, “Joint precoding and predistortion techniques for satellite telecommunication systems,” in *Wireless Communication Systems, 2005. 2nd International Symposium on*, Sept 2005, pp. 688–692.

[11] ETSI EN 302 307 V1.1.2, “Digital video broadcasting (DVB); second generation framing structure, channel coding and modulation systems for broadcasting, interactive services, news gathering and other broad-band satellite applications (DVB-S2), european broadcasting union (EBU)."

[12] E. Casini, R. D. Gaudenzi, and A. Ginesi, “DVB-S2 modem algorithms design and performance over typical satellite channels,” *International Journal of Sat. Comm. and Netw.*, vol. 22, no. 3, pp. 281–318, 2004. [Online]. Available: http://dx.doi.org/10.1002/sat.791

[13] G. Maral and M. Bousquet, *Satellite Communications systems*. Wiley, 2009.

[14] D. Christopoulos, S. Chatzinotas, and B. Ottersten, “User scheduling for coordinated dual satellite systems with linear precoding,” in *Proc. of IEEE Int. Conf. on Commun (ICC),* Budapest, Hungary, 2013.